

# A substantial population of low mass stars in luminous elliptical galaxies

Pieter G. van Dokkum<sup>1</sup> & Charlie Conroy<sup>2,3</sup>

<sup>1</sup> Astronomy Department, Yale University, New Haven, CT, USA

<sup>2</sup> Department of Astrophysical Sciences, Princeton University, Princeton, NJ, USA

<sup>3</sup> Harvard-Smithsonian Center for Astrophysics, Cambridge, MA, USA

The stellar initial mass function (IMF) describes the mass distribution of stars at the time of their formation and is of fundamental importance for many areas of astrophysics. The IMF is reasonably well constrained in the disk of the Milky Way<sup>1</sup> but we have very little direct information on the form of the IMF in other galaxies and at earlier cosmic epochs. Here we investigate the stellar mass function in elliptical galaxies by measuring the strength of the Na I doublet<sup>2,3</sup> and the Wing-Ford molecular FeH band<sup>4,5</sup> in their spectra. These lines are strong in stars with masses  $\lesssim 0.3 M_{\odot}$  and weak or absent in all other types of stars.<sup>5-7</sup> We unambiguously detect both signatures, consistent with previous studies<sup>8</sup> that were based on data of lower signal-to-noise ratio. The direct detection of the light of low mass stars implies that they are very abundant in elliptical galaxies, making up  $> 80\%$  of the total number of stars and contributing  $> 60\%$  of the total stellar mass. We infer that the IMF in massive star-forming galaxies in the early Universe produced many more low mass stars than the IMF in the Milky Way disk, and was probably slightly steeper than the Salpeter form<sup>9</sup> in the mass range  $0.1 - 1 M_{\odot}$ .

We obtained spectra of eight of the most luminous and massive galaxies in the nearby Universe: four of the brightest early-type galaxies in the Virgo cluster and four in the Coma cluster. The galaxies were selected to have velocity dispersions  $\sigma > 250 \text{ km s}^{-1}$ , and were observed with the Low-Resolution Imaging Spectrometer<sup>10</sup> (LRIS) on the Keck I telescope. In 2009 the red arm of LRIS was outfitted with fully-depleted LBNL CCDs, which have excellent sensitivity out to  $\lambda > 9000 \text{ \AA}$  and virtually no fringing. The individual spectra of the four galaxies in each of the two clusters were de-redshifted, averaged, and binned to a resolution of  $8 \text{ \AA}$ .

In Fig. 1b,c we show the spectral region near the  $\lambda\lambda 8183, 8195$  Na I doublet for the Virgo and Coma galaxies. The doublet appears as a single absorption feature due to Doppler broadening. In Fig. 1e,f we show the region around the  $\lambda 9916$  Wing-Ford band for the Virgo galaxies. This region could not be observed with sufficient signal in Coma as it is redshifted to  $1.015 \mu\text{m}$ . The spectra are of very high quality. The median  $1\sigma$  scatter of the four galaxies around the average spectrum is only  $\sim 0.3\%$  per spectral

bin. The median absolute difference between the Virgo and Coma spectra is 0.4 % per spectral bin.

Both the Na I doublet and the Wing-Ford band are unambiguously detected. The central wavelength of the observed Na I line coincides with the weighted average wavelength of the doublet and the observed Wing-Ford band has the characteristic asymmetric profile reflecting the  $A^4\Delta - X^4\Delta$  transition of FeH.<sup>5</sup> The Na I index is  $0.058 \pm 0.006$  mag in the Virgo galaxies and  $0.057 \pm 0.007$  mag in Coma. The Wing-Ford index in Virgo galaxies is  $0.027 \pm 0.005$ . The uncertainties are determined from the scatter among the individual galaxies. Note that any residual systematic problems with the detector or atmosphere are incorporated in this scatter, as the features were originally redshifted to a different observed wavelength range for each of the galaxies.

The immediate implication is that stars with masses  $\lesssim 0.3 M_{\odot}$  are present in substantial numbers in the central regions of elliptical galaxies. Such low mass stars are impossible to detect individually in external galaxies, as they are too faint: Barnard’s star would have a  $K$  band magnitude of 39 at the distance of the Virgo cluster. This in turn implies that there was a channel for forming low mass stars in the progenitors of luminous early-type galaxies in clusters. These star-forming progenitors are thought to be relatively compact galaxies at  $z = 2 - 5$  with star formation rates of 10s or 100s of Solar masses per year. Some studies have suggested truncated IMFs for such galaxies,<sup>11</sup> with a cutoff below  $1 M_{\odot}$ . Such dwarfless IMFs are effectively ruled out by the detection of the Na I line and the Wing-Ford band.

We turn to stellar population synthesis models to quantify the number of low mass stars in elliptical galaxies. As discussed in detail in the Supplementary Information, we use a flexible stellar population synthesis code<sup>12</sup> combined with an extensive empirical library of stellar near-infrared spectra.<sup>13</sup> In Fig. 1 we show synthetic spectra in both spectral regions for different choices of the IMF,<sup>1,9,14</sup> including IMFs that are steeper than the Salpeter form. The fits are excellent, with differences between data and the best-fitting model  $\lesssim 0.5\%$  over the entire spectral range. Predicted line indices are compared to the observed values in Fig. 2. The data prefer IMFs with substantial dwarf populations. The best fits are obtained for a logarithmic IMF slope of  $x \sim -3$ , a more dwarf-rich (“bottom-heavy”) IMF than even the Salpeter form, which has  $x = -2.35$ . A Kroupa IMF (which is appropriate for the Milky Way) is inconsistent with the Wing-Ford data at  $> 2\sigma$  and inconsistent with the Na I data at  $> 4\sigma$ , as are IMFs with even more suppressed dwarf populations.<sup>14–16</sup> We note that the  $x = -3$  IMF also provides a much better fit to the region around  $0.845\mu\text{m}$  than any of the other forms. Taking the Salpeter IMF as a limiting case, we find that stars with masses of  $0.1 M_{\odot} - 0.3 M_{\odot}$  make up at least 80 % of the total number of living stars in elliptical galaxies, and contribute at least 60 % of the total stellar mass.

Although the formal uncertainty in the derived IMF slope is small we stress that some unknown systematic effect could be present in the stellar population synthesis

modeling. In particular, weak features in the spectra of giant stars in elliptical galaxies may be incorrectly represented by the Milky Way giants that we use. It may also be that the Na abundance of low mass stars in elliptical galaxies is different from that of low mass mass stars in the Milky Way. The fact that all models fit the spectra of both the Virgo and Coma galaxies extremely well outside of the IMF-sensitive regions gives some confidence in our approach, and as we show in the Supplementary Information the quality of the fit constrains possible contamination of particular elements such as TiO.

Besides model uncertainties, the interpretation may be complicated by the fact that we are constraining the IMF some 10 billion years after the stars were formed. It is now generally thought that elliptical galaxies have undergone several (or many) mergers with other galaxies after their initial collapse,<sup>17</sup> which may imply that the stellar population is more complex than our single age, single metallicity model. On the other hand, these accretion events probably mostly add stars at large radii<sup>18</sup> and may not have affected the core regions very much. It will be interesting to search for gradients in dwarf-sensitive features with more extensive data.<sup>19</sup>

Our results are consistent with previous studies of the near-infrared spectra of elliptical galaxies.<sup>8,20</sup> They are also consistent with recent dynamical and lensing constraints on the IMF in elliptical galaxies with large velocity dispersions<sup>21</sup> and directly identify the stars that are responsible for their high masses: the dynamical data cannot distinguish dwarf-rich IMFs from dwarf-deficient IMFs as the latter have a large amount of mass in stellar remnants.<sup>14</sup> A steep IMF for elliptical galaxies is also qualitatively consistent with the apparently higher number of low mass stars in the Milky Way bulge than in the disk.<sup>22</sup> Our best-fitting IMF does not appear to be consistent with the observed color and  $M/L$  evolution of massive cluster galaxies,<sup>14</sup> which suggest an IMF with a slope  $x \sim 0$  around  $\sim 1 M_{\odot}$ . Interpreting the evolution of the colors and luminosities of elliptical galaxies relies on the assumption that these galaxies evolve in a self-similar way, which may not be valid.<sup>18,23</sup> It could also be that the form of the IMF is more complex than a powerlaw.

Our results also seem inconsistent with theoretical arguments for dwarf-deficient IMFs at high redshift, which have centered on the idea that the characteristic mass of stars scales with the Jeans mass in molecular clouds.<sup>24,25</sup> The Jeans mass has a strong temperature dependence and it has been argued that relatively high ambient temperatures in high-redshift star forming galaxies may have set a floor to the characteristic mass in the progenitors of elliptical galaxies.<sup>24,14</sup> However, the Jeans mass also scales with density, and the gas densities in the star-forming progenitors of the cores of elliptical galaxies were almost certainly significantly higher than typical densities of star forming regions in the Milky Way. Numerical simulations suggest that the formation of low mass stars becomes inevitable if sufficiently high densities are

reached on sub-parsec scales.<sup>26</sup> Furthermore, recent semi-analytic models of the thermal evolution of gas clouds have emphasized the effects of dust-induced cooling,<sup>27</sup> which is relatively insensitive to the ambient temperature and particularly effective at high densities. Time-scale arguments suggest that the physical conditions expected in starburst galaxies at high redshift might even enhance low-mass star formation, rather than suppress it.<sup>28</sup>

Taken at face value, our results imply that the form of the IMF is not universal but depends on the prevailing physical conditions: Kroupa-like in quiet, star-forming disks and dwarf-rich in the progenitors of massive elliptical galaxies. This informs models of star formation and has important implications for the interpretation of observations of galaxies in the early Universe. The stellar masses and star formation rates of distant galaxies are usually estimated from their luminosities, assuming some form of the IMF.<sup>29,30</sup> Our results suggest that a different form should be used for different galaxies, greatly complicating the analysis. The bottom-heavy IMF advocated here may also require a relatively low fraction of dark matter within the central regions of nearby massive galaxies.<sup>21</sup>

---

Received 2 November 2018; Accepted **draft**.

1. Kroupa, P. On the variation of the initial mass function. *Mon. Not. R. Astron. Soc.* **322**, 231–246 (2001)
2. Faber, S. M., & French, H. B. Possible M dwarf enrichment in the semistellar nucleus of M31. *Astrophys. J.*, **235**, 405–412 (1980)
3. Schiavon, R. P., Barbuy, B., Rossi, S. C. F., & Milone, A. The Near-Infrared Na I Doublet Feature in M Stars. *Astrophys. J.* **479**, 902–908 (1997)
4. Wing, R. F., & Ford, W. K. The Infrared Spectrum of the Cool Dwarf Wolf 359. *Publ. Astron. Soc. Pacific* **81**, 527–529 (1969)
5. Schiavon, R. P., Barbuy, B., & Singh, P. D. The FeH Wing-Ford Band in Spectra of M Stars. *Astrophys. J.* **484**, 499–510 (1997)
6. Schiavon, R. P., Barbuy, B., & Bruzual, A. G. Near-Infrared Spectral Features in Single-aged Stellar Populations. *Astrophys. J.* **532**, 453–460 (2000)
7. Cushing, M. C., Rayner, J. T., Davis, S. P., & Vacca, W. D. FeH Absorption in the Near-Infrared Spectra of Late M and L Dwarfs. *Astrophys. J.* **582**, 1066–1072 (2003)
8. Couture, J., & Hardy, E. The low-mass stellar content of galaxies – Constraints through hybrid population synthesis near 1 micron. *Astrophys. J.* **406**, 142–157 (1993)
9. Salpeter, E. E. The Luminosity Function and Stellar Evolution. *Astrophys. J.* **121**, 161–167 (1955)
10. Oke, J. B., Cohen, J. G., Carr, M., Cromer, J., Dingizian, A. *et al.* The Keck Low-Resolution Imaging Spectrometer. *Publ. Astron. Soc. Pacific* **107**, 375–385 (1995)

11. Baugh, C. M., Lacey, C. G., Frenk, C. S., Granato, G. L., Silva, L. *et al.* Can the faint submillimetre galaxies be explained in the  $\Lambda$  cold dark matter model? *Mon. Not. R. Astron. Soc.* **356**, 1191–1200 (2005)
12. Conroy, C., Gunn, J. E., & White, M. The Propagation of Uncertainties in Stellar Population Synthesis Modeling. I. The Relevance of Uncertain Aspects of Stellar Evolution and the Initial Mass Function to the Derived Physical Properties of Galaxies. *Astrophys. J.* **699**, 486–506 (2009)
13. Rayner, J. T. and Cushing, M. C. and Vacca, W. D. The Infrared Telescope Facility (IRTF) Spectral Library: Cool Stars. *Astrophys. J.* **623**, 289–432 (2009)
14. van Dokkum, P. G. Evidence of Cosmic Evolution of the Stellar Initial Mass Function. *Astrophys. J.* **674**, 29–50 (2008)
15. Fardal, M. A., Katz, N., Weinberg, D. H., & Davé, R. On the evolutionary history of stars and their fossil mass and light. *Mon. Not. R. Astron. Soc.* **379**, 985–1002 (2007)
16. Davé, R. The galaxy stellar mass-star formation rate relation: evidence for an evolving stellar initial mass function? *Mon. Not. R. Astron. Soc.* **385**, 147–160 (2008)
17. Naab, T., Johansson, P. H., Ostriker, J. P., & Efstathiou, G. Formation of Early-Type Galaxies from Cosmological Initial Conditions. *Astrophys. J.* **658**, 710–720 (2007)
18. van Dokkum, P. G., Whitaker, K. E., Brammer, G., Franx, M., Kriek, M., *et al.* The Growth of Massive Galaxies Since  $z = 2$ . *Astrophys. J.* **709**, 1018–1041 (2010)
19. Boroson, T. A., & Thompson, I. B. Color distributions in early type galaxies. III – Radial gradients in spectral features. *Astron. J.* **101**, 111–126 (1991)
20. Cenarro, A. J., Gorgas, J., Vazdekis, A., Cardiel, N., & Peletier, R. F. Near-infrared line-strengths in elliptical galaxies: evidence for initial mass function variations? *Mon. Not. R. Astron. Soc.* **339**, L12–L16 (2003)
21. Treu, T., Auger, M. W., Koopmans, L. V. E., Gavazzi, R., Marshall, P. J., & Bolton, A. S. The Initial Mass Function of Early-Type Galaxies. *Astrophys. J.* **709**, 1195–1202 (2010)
22. Calchi Novati, S., de Luca, F., Jetzer, Ph., Mancini, L., & Scarpetta, G. Microlensing constraints on the Galactic bulge initial mass function. *Astron. Astrophys.*, **480**, 723–733
23. van der Wel, A., Holden, B. P., Zirm, A. W., Franx, M., Rettura, A., Illingworth, G. D., & Ford, H. C. Recent Structural Evolution of Early-Type Galaxies: Size Growth from  $z = 1$  to  $z = 0$ . *Astrophys. J.*, **688**, 48–58
24. Larson, R. B. Thermal physics, cloud geometry and the stellar initial mass function. *Mon. Not. R. Astron. Soc.* **359**, 211–222 (2005)
25. Bate, M. R., & Bonnell, I. A. The origin of the initial mass function and its dependence on the mean Jeans mass in molecular clouds. *Mon. Not. R. Astron. Soc.* **356**, 1201–1221 (2005)

26. Bonnell, I. A., Clark, P., & Bate, M. R. Gravitational fragmentation and the formation of brown dwarfs in stellar clusters. *Mon. Not. R. Astron. Soc.* **389**, 1556–1562 (2008)
27. Schneider, R., & Omukai, K. Metals, dust and the cosmic microwave background: fragmentation of high-redshift star-forming clouds. *Mon. Not. R. Astron. Soc.* **402**, 429–435 (2010)
28. Banerji, S., Viti, S., Williams, D. A., & Rawlings, J. M. C. Timescales for Low-Mass Star Formation in Extragalactic Environments: Implications for the Stellar Initial Mass Function. *Astrophys. J.* **692**, 283–289 (2009)
29. Marchesini, D., van Dokkum, P. G., Förster Schreiber, N. M., Franx, M., Labbé, I., & Wuyts, S. The Evolution of the Stellar Mass Function of Galaxies from  $z = 4.0$  and the First Comprehensive Analysis of its Uncertainties: Evidence for Mass-Dependent Evolution. *Astrophys. J.* **701**, 1765–1796 (2009)
30. Labbé, I., González, V., Bouwens, R. J., Illingworth, G. D., Franx, M., Trenti, M., Oesch, P. A., et al. Star Formation Rates and Stellar Masses of  $z = 7.8$  Galaxies from IRAC Observations of the WFC3/IR Early Release Science and the HUDF Fields. *Astrophys. J.* **716**, L103–L108 (2010)

---

**Supplementary Information** is linked to the online version of the paper at [www.nature.com/nature](http://www.nature.com/nature).

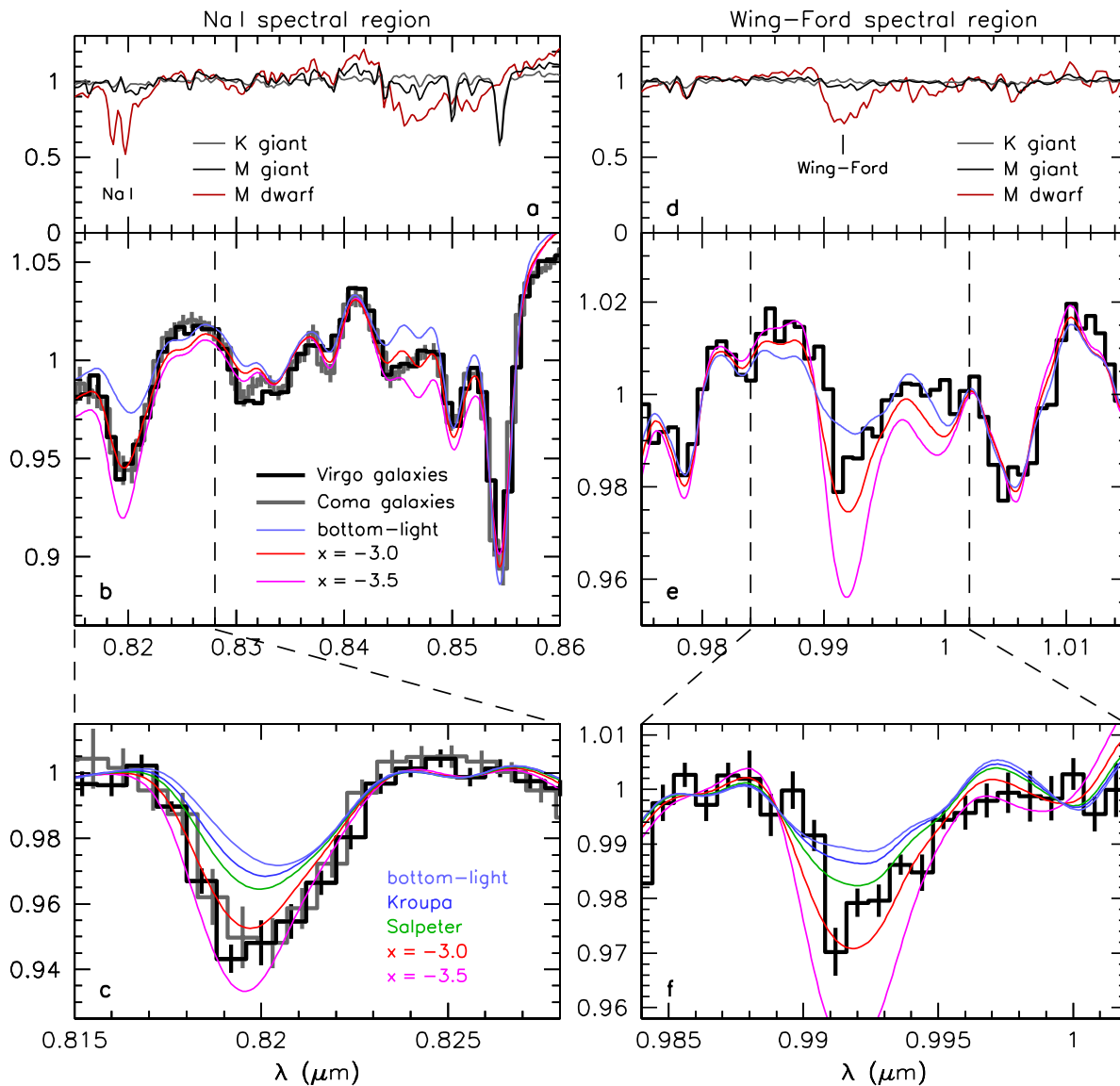
**Acknowledgements** We thank Rachel Bezanson, Jarle Brinchmann, Richard Larson, and Bob Zinn for discussions. We thank Ricardo Schiavon for insightful comments which greatly improved the manuscript. This study is based on observations obtained at the W. M. Keck Observatory. The authors wish to recognize and acknowledge the very significant cultural role and reverence that the summit of Mauna Kea has always had within the indigenous Hawaiian community. We are most fortunate to have the opportunity to conduct observations from this mountain.

**Author Contributions** P.v.D. obtained and analyzed the data and contributed to the analysis and interpretation. C.C. constructed the stellar population synthesis models and contributed to the analysis and interpretation.

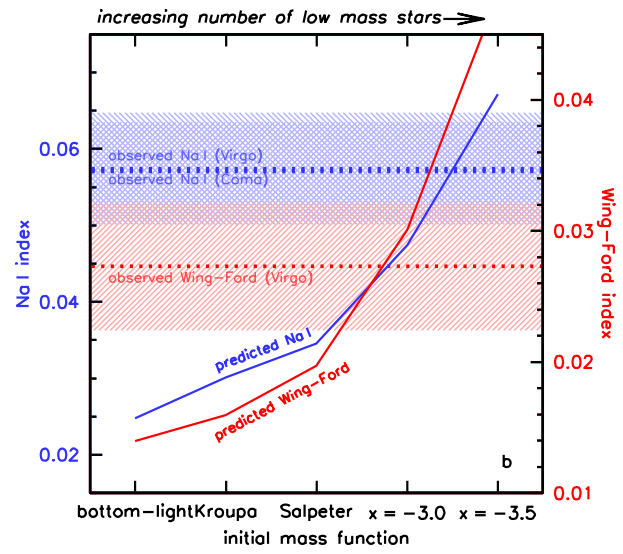
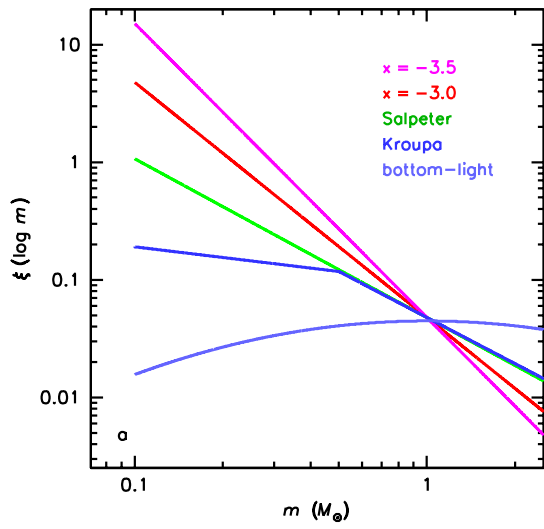
**Author Information** Reprints and permissions information is available at [npg.nature.com/reprintsandpermissions](http://npg.nature.com/reprintsandpermissions). Correspondence and requests for materials should be addressed to P.v.D. ([pieter.vandokkum@yale.edu](mailto:pieter.vandokkum@yale.edu)).

**Figure 1 | Detection of the Na I doublet and the Wing-Ford band.** **a**, Spectra in the vicinity of the  $\lambda\lambda 8183, 8195$  Na I doublet for three stars from the IRTF library:<sup>12</sup> a K0 giant, which dominates the light of old stellar populations; an M6 dwarf, whose (small) contribution to the integrated light is sensitive to the form of the IMF at low masses; and an M3 giant, which has potentially contaminating TiO spectral features in this wavelength range. **b**, Averaged Keck/LRIS spectra of NGC 4261, NGC 4374, NGC 4472, and NGC 4649 in the Virgo cluster (black line) and NGC 4840, NGC 4926, IC 3976, and NGC 4889 in the Coma cluster (grey line). Four exposures of 180 s were obtained for each galaxy. The one-dimensional spectra were extracted from the reduced two-dimensional data by summing the central  $4''$ , which corresponds to  $\approx 0.4$  kpc at the distance of Virgo and  $\approx 1.8$  kpc at the distance of Coma. We found little or no dependence of the results on the choice of aperture. Colored lines show stellar population synthesis models for a dwarf-deficient “bottom-light” IMF,<sup>14</sup> a dwarf-rich “bottom-heavy” IMF with  $x = -3$ , and an even more dwarf-rich IMF. The models are for an age of 10 Gyr and were smoothed to the average velocity dispersion of the galaxies. The  $x = -3$  IMF fits the spectrum remarkably well. **c**, Spectra and models around the dwarf-sensitive Na I doublet. A Kroupa IMF, which is appropriate for the Milky Way, does not produce a sufficient number of low mass stars to explain the strength of the absorption. An IMF steeper than Salpeter appears to be needed. **d,e,f**, Spectra and models near the  $\lambda 9916$  Wing-Ford band. The observed Wing-Ford band also favors an IMF that is more abundant in low mass stars than the Salpeter IMF. All spectra and models were normalized by fitting low order polynomials (excluding the feature of interest). The polynomials were quadratic in **a,b,d,e** and linear in **c,f**.

**Figure 2 | Constraining the IMF.** **a**, Various stellar IMFs, ranging from a “bottom-light” IMF with strongly suppressed dwarf formation<sup>14</sup> (light blue) to an extremely “bottom-heavy” IMF with a slope  $x = -3.5$ . The IMFs are normalized at  $1 M_{\odot}$ , as stars of approximately that mass dominate the light of elliptical galaxies. **b**, Comparison of predicted line Na I and Wing-Ford indices to the observed values. The indices were defined analogous to refs. 4 and 8. The Na I index has central wavelength  $0.8195 \mu$  and side bands at  $0.816 \mu\text{m}$  and  $0.825 \mu\text{m}$ . The Wing-Ford index has central wavelength  $0.992 \mu\text{m}$  and side bands at  $0.985 \mu\text{m}$  and  $0.998 \mu\text{m}$ . The central bands and side bands are all  $20 \text{ \AA}$  wide. Both observed line indices are much stronger than expected for a Kroupa IMF. The best fits are obtained for IMFs that are slightly steeper than Salpeter.







### Supplementary Information: Stellar population synthesis modeling

The stellar population model used in the present analysis was constructed specifically for this project. We therefore describe it in some detail below.

#### *Construction of the model:*

The IRTF spectral library<sup>1,2</sup> constitutes the core of our model. This spectral library is novel in its near-IR coverage of a large sample of cool stars at a resolving power of  $R \sim 2000$ . 65 stars were selected from this library with luminosity classes III and V (giants and dwarfs). Peculiar stars were removed, including stars with non-solar Fe abundance and/or other peculiar abundance patterns (mainly Ca, CN, CH, and Ba), as well as known pulsating M giants. Stars with significant reddening were also removed. The IRTF library includes 2MASS *JHK* and literature *V* band photometry for each star.

We estimated effective temperatures for these stars based on empirical  $V - K$  vs.  $T_{\text{eff}}$  relations that have been separately determined for giants<sup>3-5</sup> and dwarfs.<sup>6,7</sup> The adopted dwarf relations agree to within 100 K with a recently updated temperature scale.<sup>8,9</sup>

The IRTF library is absolute-flux calibrated against 2MASS photometry. We adopt parallax values obtained from SIMBAD in order to derive absolute luminosities. In order to derive bolometric luminosities, which we will use to assign stellar masses, we must extrapolate the IRTF library beyond the observed range. We perform the extrapolation by utilizing the latest version of the PHOENIX model spectra. The model spectra are normalized to the IRTF library at the blue and red ends of the observed wavelength range so that the extrapolation is continuous across the transition region. The model spectrum used to extrapolate each IRTF stellar spectrum was chosen from the estimated  $T_{\text{eff}}$  for each IRTF star and an estimate of the surface gravity of the star based on its luminosity class. We note that the extrapolation does not lead to large uncertainties as the IRTF wavelength range ( $0.8 - 2.5 \mu\text{m}$ ) encompasses the majority of the bolometric flux, especially for K and M stars. As an example, 80 % of the flux from M-type stars is emitted within the IRTF spectral range.

The resulting  $T_{\text{eff}}$  and  $L_{\text{bol}}$  for each IRTF star is plotted in Supp. Fig. 1. Also shown in this Figure are model isochrones (described below). The agreement between the data and models is remarkable, and provides a valuable consistency check on both the estimated  $T_{\text{eff}}$  and  $L_{\text{bol}}$  values.

We adopt a combination of isochrones in order to utilize the most accurate stellar models for each range in stellar mass. At the lowest masses we adopt the Baraffe stellar evolution calculations,<sup>10</sup> which are unique in their use of realistic atmospheric boundary conditions. Between  $0.2 M_{\odot}$  and the tip of the RGB we use the Dartmouth evolutionary calculations,<sup>11</sup> which have been shown to produce accurate fits to photometry of open and globular clusters of a variety of ages and metallicities.<sup>12</sup> The Padova evolutionary tracks<sup>13</sup> are used to extend the isochrones through the horizontal branch and asymptotic giant branch evolutionary phases. This combined isochrone set is shown in Supp. Fig. 1.

The isochrones are used to assign masses to each IRTF spectrum, based on the measured  $L_{\text{bol}}$  for each star. We note that the stellar  $T_{\text{eff}}$  values are used only to choose the appropriate PHOENIX model spectra to extrapolate the observed spectra. Our conclusions remain unchanged if we instead assign masses based on the estimated  $T_{\text{eff}}$  for each star. Alpha-enhancements of 0.2 dex have a very minor effect on the  $L_{\text{bol}} - M$  and  $T_{\text{eff}} - M$  relations, when  $[\text{Fe}/\text{H}]$  is held constant. As a final test of our procedure we compare the masses to those

predicted from empirical relations between mass and  $K$ -band luminosity derived for stars in binary systems.<sup>14,15</sup> Such relations are completely independent of stellar evolution calculations because the masses are derived from dynamical modeling. The stellar mass –  $K$ -band luminosity relation for our IRTF stars agrees very well with the relations based on dynamical masses in the range  $0.08 < M < 0.6 M_{\odot}$ . The agreement is particularly strong when bolometric luminosities are used to assign masses, which motivates the use of bolometric luminosities as our default method. Based on these comparisons, we conclude that our mass estimates are reliable.

Once masses are assigned, a synthesized spectrum is created by integrating the observed spectra over an initial mass function.

*Metallicity and  $\alpha$ -enhancement:*

The empirical spectral library that we use has important advantages over libraries of model atmospheres. Model atmospheres do not reproduce molecular features such as TiO very well, which makes it difficult to interpret fits of these models to our spectra. We note here that Kurucz models — which are used in most existing stellar population synthesis models at  $\lambda > 8000 \text{ \AA}$  — also prefer IMFs that are more “bottom-heavy” than the Kroupa IMF, but give much poorer fits than the IRTF empirical library to the spectral regions away from Na I and the Wing-Ford band.

A disadvantage of the empirical library is that it is not straightforward to assess the effects of abundance variations. We know that the iron abundance in the eight Coma and Virgo ellipticals is approximately Solar,<sup>16,17</sup> and so the value of  $[\text{Fe}/\text{H}]$  of the Milky Way stars is appropriate for the galaxies that we study here. However, the abundance of  $\alpha$ -elements (and the overall mass-weighted metallicity  $[\text{Z}/\text{H}]$ ) is higher in massive elliptical galaxies than in the Milky Way stars. Although sodium (responsible for the Na I line) and iron (responsible for the Wing-Ford band) are themselves not  $\alpha$ -elements, both lines and their sidebands overlap with TiO lines that are present in M giants.

We empirically determined to what extent enhanced TiO absorption could influence the results by creating models with artificially enhanced late M giant light. The model shown in Supp. Fig. 2 has a Kroupa IMF and an additional contribution of late M giants amounting to 40% of the light at  $0.9 \mu\text{m}$ . This is an extreme model as these stars should contribute only a few percent to the light, but we use it here to assess the effects of enhancing TiO features. This model fits the observed strength of the Wing-Ford band quite well as it coincides with the  $\delta(2 - 3)$  band of TiO. However, it also predicts that other TiO features are nearly as strong as the absorption at  $0.99 \mu\text{m}$ , which is clearly not the case. Moreover, the fit to the Na I line is not improved as the only relevant TiO feature is slightly redward of Na I, and the fit to the rest of the spectrum in the wavelength range  $0.815 - 0.860 \mu\text{m}$  is unacceptable. We note that the apparently limited enhancement of TiO with respect to the Milky Way giants is consistent with the weak response of TiO to either metallicity or  $\alpha$ -enhancement in the PHOENIX library and the models of ref. 18.

We infer that the Wing-Ford band should be interpreted with caution but that the combination of the Wing-Ford band with TiO features at other wavelengths and (particularly) the Na I line should be a robust indicator of the presence of low mass stars. This is fully consistent with previous theoretical work.<sup>19</sup>

Received 2 November 2018; Accepted **draft**.

1. Cushing, M. C., Rayner, J. T., & Vacca, W. D. An Infrared Spectroscopic Sequence of M, L, and T Dwarfs. *Astrophys. J.* **623**, 1115–1140 (2005)
2. Rayner, J. T., Cushing, M. C., & Vacca, W. D. The Infrared Telescope Facility (IRTF) Spectral Library: Cool Stars. *Astrophys. J.* **623**, 289–432 (2009)
3. Alonso, A., Arribas, S., & Martínez-Roger, C. The effective temperature scale of giant stars (F0-K5). II. Empirical calibration of  $T_{\text{eff}}$  versus colours and [Fe/H]. *Astron. Astrophys.* **140**, 261–277 (1999)
4. Perrin, G., Coudé du Foresto, V., Ridgway, S. T., Mariotti, J.-M., Traub, W. A., Carleton, N. P., & Lacasse, M. G. Extension of the effective temperature scale of giants to types later than M6. *Astron. Astrophys.* **331**, 619–626 (1998)
5. Ridgway, S. T., Joyce, R. R., White, N. M., & Wing, R. F. Effective temperatures of late-type stars - The field giants from K0 to M6. *Astrophys. J.* **235**, 126–137 (1980)
6. Alonso, A., Arribas, S., & Martinez-Roger, C. The empirical scale of temperatures of the low main sequence (F0V-K5V). *Astron. Astrophys.* **313**, 873–890 (1996)
7. Leggett, S. K., Allard, F., Berriman, G., Dahn, C. C., & Hauschildt, P. H. Infrared Spectra of Low-Mass Stars: Toward a Temperature Scale for Red Dwarfs. *Astrophys. J.* **104**, 117 (1996)
8. Casagrande, L., Flynn, C., & Bessell, M. M dwarfs: effective temperatures, radii and metallicities. *Mon. Not. R. Astron. Soc.* **389**, 585–607 (2008)
9. Casagrande, L., Ramírez, I., Meléndez, J., Bessell, M., & Asplund, K. An absolutely calibrated  $T_{\text{eff}}$  scale from the infrared flux method. Dwarfs and subgiants. *Mon. Not. R. Astron. Soc.* **512**, 54 (2010)
10. Baraffe, I., Chabrier, G., Allard, F., & Hauschildt, P. H. Evolutionary models for solar metallicity low-mass stars: mass-magnitude relationships and color-magnitude diagrams. *Astron. Astrophys.* **337**, 403–412 (1998)
11. Dotter, A., Chaboyer, B., Jevremović, D., Kostov, V., Baron, E., & Ferguson, J. W. The Dartmouth Stellar Evolution Database. *Astrophys. J. Supp.* **178**, 89–101 (2008)
12. An, D., Pinsonneault, M. H., Masseron, T., Delahaye, F., Johnson, J. A., Terndrup, D. M., Beers, T. C., Ivans, I. I., & Ivezić, Ž Galactic Globular and Open Clusters in the Sloan Digital Sky Survey. II. Test of Theoretical Stellar Isochrones. *Astrophys. J.* **623**, 523–544 (2009)
13. Marigo, P., Girardi, L., Bressan, A., Groenewegen, M. A. T., Silva, L., & Granato, G. L. Evolution of asymptotic giant branch stars. II. Optical to far-infrared isochrones with improved TP-AGB models. *Astron. Astrophys.* **482**, 883–905 (2008)
14. Henry, T. J. & McCarthy, Jr., D. W. The mass-luminosity relation for stars of mass 1.0 to 0.08 solar mass. *Astron. J.* **106**, 773–789 (1993)

15. Delfosse, X., Forveille, T., Ségransan, D., Beuzit, J.-L., Udry, S., Perrier, C., & Mayor, M. Accurate masses of very low mass stars. IV. Improved mass-luminosity relations. *Astron. Astrophys.* **364**, 217–224 (2000)
  16. Trager, S. C., Faber, S. M., Worthey, G., & González, J. J. The Stellar Population Histories of Local Early-Type Galaxies. I. Population Parameters. *Astrophys. J.* **119**, 1645–1676 (2000)
  17. Thomas, D., Maraston, C., Bender, R., & Mendes de Oliveira, C. The Epochs of Early-Type Galaxy Formation as a Function of Environment. *Astrophys. J.* **621**, 673–694 (2005)
  18. Thomas, D., Maraston, C., & Bender, R. Stellar Population models of Lick indices with variable element abundance ratios. *Mon. Not. R. Astron. Soc.* **339**, 897–911 (2003)
  19. Schiavon, R. P., Barbuy, B., Rossi, S. C. F., & Milone, A. The Near-Infrared Na I Doublet Feature in M Stars. *Astrophys. J.* **479**, 902–908 (1997)
-

**Supplementary Figure 1 | The IRTF stellar library.** Hertzsprung-Russell diagram of IRTF stars and theoretical stellar evolution calculations. IRTF stellar  $L_{\text{bol}}$  and  $T_{\text{eff}}$  have been estimated as described in the text. Theoretical models assume  $[\text{Fe}/\text{H}] = 0.0$  and an age of 13.7 Gyr. The models encompass all phases of stellar evolution from main sequence hydrogen burning through the end of the asymptotic giant branch, and extend down to the hydrogen burning limit of  $0.08 M_{\odot}$ .

**Supplementary Figure 2 | Effect of enhancing M giant features.** **a** Spectra and models around the Na I doublet. Our favored model with a steep IMF ( $x = -3.0$ ) is compared to a model that assumes a Kroupa IMF with the addition of a 40% light contribution from an M6 giant star. Since late M giants have very strong TiO features this exercise is meant to mimic the effects of increasing  $\alpha$ -enhancement in the models. Clearly the addition of a substantial amount of M giant light provides a poor fit to the absorption line at  $\approx 0.82 \mu\text{m}$  as the central wavelength is not matched. This demonstrates that this feature is due to Na I and not TiO. The fit is also very poor to the rest of the spectrum in this wavelength range. **b** Spectra and models around the Wing-Ford band. Here the addition of M giant light adequately reproduces the strong observed Wing-Ford absorption due to the TiO absorption feature that coincides with the FeH absorption. However, this fit also predicts unacceptably large absorption at  $0.983 \mu\text{m}$ ,  $1.001 \mu\text{m}$ , and  $1.006 \mu\text{m}$  as these TiO features are nearly as strong as the one at  $0.992 \mu\text{m}$ .

